Methods xxx (2015) xxx–xxx

Contents lists available at ScienceDirect

Methods

journal homepage: www.elsevier.com/locate/ymeth

Designing BRET-based conformational biosensors for G protein-coupled receptors

Rory Sleno, Darlaine Pétrin, Dominic Devost, Eugénie Goupil, Alice Zhang, Terence E. Hébert *

Department of Pharmacology and Therapeutics, McGill University, Canada

ARTICLE INFO

Article history:
Received 2 April 2015
Received in revised form 30 April 2015
Accepted 2 May 2015
Available online xxxx

Keywords:
Biosensor
G protein-coupled receptor
Biased signaling
Screening
Resonance energy transfer

ABSTRACT

Ligand-biased signaling is starting to have significant impact on drug discovery programs in the pharmaceutical industry and has reinvigorated our understanding of pharmacological efficacy. As such, many investigators and screening campaigns are now being directed at a larger section of the signaling responses downstream of an individual G protein-coupled receptor. Many biosensor-based platforms have been developed to capture signaling signatures. Despite our growing ability to use such signaling signatures, we remain hampered by the fact that signaling signatures may be particular to an individual cell type and thus our platforms may not be portable from cell to cell, necessitating further cell-specific biosensor development. Here, we provide a complementary strategy based on capturing receptor-proximal conformational profiles using intra-molecular BRET-based sensors composed of a *Renilla* luciferase donor engineered into the carboxy-terminus and CCPGCC motifs which bind fluorescent hairpin arsenical dyes engineered into different positions in intracellular loop 3 of FP, the receptor for PGF2α. We discuss the design and optimization of such sensors for orthosteric and allosteric ligands.

© 2015 Elsevier Inc. All rights reserved.

1. Introduction

The concept of ligand bias has re-energized current approaches to drug discovery [1–3]. Current tools to assess ligand bias in G protein-coupled receptors (GPCRs) are generally focused on the downstream signaling outputs from the receptor [4–8]. Assessment of individual signaling pathways by means of biosensors, imaging or biochemical assays has driven our understanding of the phenomena and have characterized, in some cases, the unique signaling profiles associated with different ligands for the same GPCR. These assays, though powerful, have limitations with respect to the generalization of proposed ligand signatures from cell type to cell type. Since these assays focus on downstream signaling events, they are cell or tissue context-dependent whereby the results in one cellular background may not translate to others. Every cell may have a distinct (or partially distinct) coterie of signaling pathways downstream of a given receptor. Further, assays which capture and stratify more proximal impacts of different ligands upon binding to a receptor would provide information on the earliest events at the origin of biased responses.

GPCRs are conformationally dynamic proteins even when compared to other cell surface receptors. The 7 transmembrane spanning domains linked by flexible loops and N- and C-terminal domains with minimal secondary structure provide the freedom for the receptor to sample a large spectrum of conformations in response to orthosteric ligands or allosteric modulators. It is this conformational pliability that has been proposed to underlie the mechanistic basis of biased signaling in the GPCR superfamily of cell surface receptors [2,9].

The development of tools to report protein conformational dynamics has expanded beyond the typical “snapshots” obtained using techniques that investigate protein structure such as X-ray crystallography and NMR. Further, although both these techniques have provided significant insight into receptor structure they are not amenable to high throughput and cannot yet or easily be used for drug screening [10–12]. The use of resonance energy transfer (RET) as a means to capture relative changes in conformation in a protein in a live cell is now well established [13]. Early strategies used fluorescent protein adducts such as YFP and CFP as donor and acceptor moieties but the development and use of targeted small fluorescent probes such as fluorescein arsenical hairpin binder (FlAsH) has greatly increased the power of the technology as smaller probes are more easily accommodated into protein structure [14]. The use of FlAsH as a RET acceptor has generated greater possibilities for acceptor positioning due to this reduced disruption

* Corresponding author at: Department of Pharmacology and Therapeutics, McGill University, Room 1303 McIntyre Medical Sciences Building, 3655 Promenade Sir William Osler, Montréal, Québec H3G 1Y6, Canada.
E-mail address: terence.hebert@mcgill.ca (T.E. Hébert).

http://dx.doi.org/10.1016/j.ymeth.2015.05.003
1046-2023/© 2015 Elsevier Inc. All rights reserved.

of protein structure. Previous biosensors have mostly relied on Förster resonance energy transfer (FRET) assessed by microscopy to capture the relative changes in receptor conformation upon ligand binding [15,16]. Though FRET microscopy has its advantages, namely the ability to examine individual cells and obtain subcellular resolution while benefitting from fast perfusion systems to resolve temporal events, other RET technologies are better suited for drug screening purposes [17]. The use of FlAsH-bioluminescence resonance energy transfer (BRET) has been previously reported but these sensors initially used inter-molecular donor and acceptor pairs which showed little response to agonist in the context of a D4 dopamine/β_2AR heterodimer [18]. Here, we develop a strategy to generate conformation-sensitive biosensors using intra-molecular FlAsH-BRET, a RET technology amenable to high throughput screening, which can capture robust conformational information in 96-well (or larger) formats.

Using the F prostanoid receptor (FP) as a starting point, we generated a panel of sensors, investigating conformational changes in the third intracellular loop (ICL3). By "walking" the FlAsH acceptor through different positions in ICL3, we generated a panel with a higher resolution of conformational dynamics than previously reported with this technology. This paper will present and discuss the development of these new sensors and demonstrate their ability to capture conformational information imparted by orthosteric ligands and the biased allosteric modulator PDC113.824 [19].

2. Material and methods

2.1. Reagents

Unless noted otherwise, all chemicals were reagent-grade and purchased from Sigma–Aldrich. PDC113.824 was a generous gift from Dr. William Lubell at the Université de Montréal.

2.2. Cell culture

HEK 293 cells were cultured in Dulbecco's Modified Eagle's medium supplemented with 10% vol/vol fetal bovine serum from Wisent at 37 °C in a humidified atmosphere at 95% air and 5% CO_2. Stock cells were grown to ~80% confluence in T75 flasks from Corning at which point they were plated for transfection.

2.3. Generation of FP homology model

The free web-based protein homology/analogy recognition engine V 2.0 (Phyre^2) [20] was used to generate the model based on the human FP isoform A amino acid sequence (NCBI Reference Sequence: NP_000950.1). The highest ranked model was based on the A_{2A}-adenosine receptor bound to the antagonist ZM241385 (PDB: 3EML) with a confidence of 100 and a percent I.D. of 18. The coordinates of the model were downloaded and viewed in Pymol where different regions of interest were highlighted by the coloration of specific amino acid residues in a cartoon representation.

2.4. Generation of tetracysteine-tagged receptors

To generate the inter-molecular constructs (FP containing a single tetracysteine (TC) tag), overlap extension PCR was used to introduce the TC tag (CCPGCC) at different locations in the third intracellular loop (ICL3) of the receptor coding sequences. Briefly, HA-FP was amplified by PCR using the vector pIRESpuro3-HA-FP available in our laboratory. While the 3′ ends of the primers used for first round reactions were complementary to the template DNA, the sequence 5′-tgctgccccggctgctgc-3′ (human preferred codons for CCPGCC) was added at their 5′ ends (primers were synthesized by Integrated DNA Technologies Coralville, IA). Fragments generated were mixed and allowed to anneal, and served in a second round PCR to generate a full receptor coding sequence with a TC tag inserted at one of the different positions. In our case, the positions selected for insertion of the tag were 3 or 4 amino acids apart and the loop regions were determined based on theoretical information (GPCR Natural Variant database, http://nava.liacs.nl/cgi-bin/gpcr.py?acc=P43088). All sequences were then verified using bidirectional sequencing (Génome Québec). The HA tag at the N-terminus was maintained to facilitate detection of the receptor by immunoblotting or immunocytochemistry.

To generate the intra-molecular constructs (FP containing both a TC tag in ICL3 and a modified *Renilla* luciferase (RLucII) moiety fused to the C-terminus), the inter-molecular constructs described above were used as starting points. Briefly, by PCR, a signal peptide was added to the 5′ end of the receptor just upstream of the HA tag and the stop codon was removed. This product was then inserted into the vector pcDNA3.1(-). To generate the RLucII fusion, a RLucII construct was used as template for a PCR to introduce compatible restriction sites 5′ and 3′ of the RLucII as well as a ridged linker between the 5′ restriction site and the start codon of RLucII. This product was then inserted into the pcDNA3.1(-)-FP plasmid by means of compatible restriction sites (all restriction enzymes were from New England Biolabs). Constructs were named based on the order of the TC position in ICL3 or WT for the control construct with only the RLucII moiety fused to the C-terminus. All construct sequences were then verified by bidirectional sequencing (Génome Québec).

The intra-molecular SP-HA-FP-P2 ICL3-RLucII construct was generated differently since the inter-molecular construct could not be generated as discussed below. A gene fragment was synthesized containing the appropriate TC tag insertion and compatible restriction sites at the 5′ and 3′ ends (gBlock products from Integrated DNA Technologies). The FP-WT ICL3-RLucII construct was then digested with the same restriction enzymes and the gene fragment was ligated into the backbone. The sequence was then verified by bidirectional sequencing (Génome Québec).

2.5. Other constructs

The FP-RLuc construct using in the receptor-receptor inter-molecular BRET sensor configuration was previously published as a BRET donor [21]. The Gγ_2-RLuc in the receptor-G protein inter-molecular BRET sensor configuration was also previously published as a BRET donor [22].

2.6. Validation of biosensor localization and function

2.6.1. Expression and cellular localization of recombinant receptors: immunofluorescence

For the inter-molecular biosensors, HEK 293 cells were plated on glass coverslips and transfected with 2 μg of wild type (WT) or recombinant plasmid DNA using lipofectamine 2000 (Invitrogen) following the manufacturer's instructions. Forty-eight hours post-transfection, cells were fixed with 4% paraformaldehyde (PFA) for 1 min and incubated for 10 min in ice-cold methanol (Fisher Scientific) to permeabilize the cells. Following three washes with 1× phosphate buffer saline (PBS), samples were blocked for 1 h in PBS containing 1% bovine serum albumin (BSA) fraction V (Fisher Scientific) and then incubated with the monoclonal mouse anti-HA antibody (Covance, 1:100) followed by Alexa fluor 488-conjugated secondary antibody (Invitrogen, 1:500) and DAPI, 1:5000 from a 1 mg/ml stock, as a nuclear counterstain. Cells were visualized using a Zeiss LSM-510 Meta laser-scanning microscope (63 × glycerol/water immersion

lens, Carl Zeiss, Thornwood, NY) using 488 nm/505 to 530 nm band pass (BP) filters for excitation/emission.

For the intra-molecular biosensors, HEK 293 cells were plated on 6-well plates (Costar 3516) 24 h prior to transfection. The next day, cells were transfected with 1 μg of the FP construct or pcDNA3.1(-). Lipofectamine 2000 was again used for transfection following the manufacturer's instructions. The following day, cells were detached with 0.25% Trypsin–EDTA (Wisent) and re-plated on poly-ornithine-treated black clear bottom 96-well plates (Costar 3904). Twenty-four hours later, the cells were fixed with 2% PFA for 10 min at 4 °C. To minimize non-specific binding of the antibodies, cells were blocked with a 2% BSA (Fisher Scientific) in PBS solution for 1 h at room temperature and then treated with an anti-HA primary antibody (Covance, 1:200) followed by an Alexa fluor 488-conjugated secondary antibody (Invitrogen, 1:500) and Hoechst DNA stain, diluted 1:1000 from a 1 mg/ml stock. Images were captured using an Operetta High Content Imaging system with a 20× WD objective (Perkin Elmer). Signal from Alexa fluor 488 was excited with a 475/15 filter and emission was captured with a 525/25 filter. Signal from the Hoechst DNA stain was excited with a 380/20 filter and emission was captured with a 445/35 filter.

2.6.2. Assessing functionality of recombinant receptors: ERK1/2 activation

HEK 293 cells were plated in 12-well plates (Costar 3513) and transiently transfected with WT or the various recombinant receptor constructs using lipofectamine 2000. Forty-eight hours post-transfection, cells were treated with 1 μM of receptor agonist, PGF2α, for 5 min, then lysed in 250 μl 1× Laemmli buffer (2% SDS, 10% glycerol, 60 mM Tris pH 6.8, 0.02% bromophenol blue, 5% β-mercaptoethanol). Samples were sonicated for 10 s, heated to 95 °C for 5 min and analyzed using SDS–PAGE. Anti-p44/42 antibody (Cell Signaling Technology #9101) was used to detect phospho-ERK while ERK 1 antibody (K-23) (Santa Cruz sc-94) was used to control for equal loading. A secondary anti-rabbit antibody conjugated to horseradish peroxidase was used to visualize the bands by chemiluminescence.

2.7. FlAsH labeling

For the inter-molecular constructs, the FlAsH labeling procedure was done using HEK 293 cells plated in 12-well plates (Costar 3513) and transfected with a 1:1 ratio of each plasmid (as described above) used to generate the bimolecular sensors using lipofectamine 2000. If possible, it is useful to titrate expression such that each is expressed equally, perhaps by marking them with distinct epitope tages. Forty-eight hours post-transfection, samples were labeled according to the following procedure. First, to prepare the FlAsH-ETD_2 solution, one volume of 2 mM FlAsH reagent (Invitrogen) was incubated for 5–10 min at room temperature with two volumes of 25 mM 1,2-ethanedithiol (EDT), obtained by diluting the 12 M stock solution in dimethylsulfoxide (DMSO). Note that EDT (in addition to being toxic) has a very characteristic (and strong) odor and all work should be done under a fume hood. 100 μl of Hank's Balanced Salt Solution (HBSS, Wisent) was added to the 667 μM FlAsH-ETD_2 solution, mixed well and incubated for 5 min. The 100 μl was further diluted in the remaining working volume of HBSS, taking into consideration that 500 μl were needed per well when working with cells in 12-well plates (Costar 3513). The working labeling solution was finally composed of 750 nM FlAsH and 18.7 μM EDT. Once the FlAsH-ETD_2 labeling solution was prepared, cells were washed twice in HBSS and incubated with the labeling solution for 1 h at 37 °C, where plates were covered and sealed with parafilm, protected from light. After removing the FlAsH-ETD_2 labeling solution, cells were incubated in a 100 μM 2,3-dimercapto-1-propanol (BAL) diluted in HBSS wash buffer for 10 min at 37 °C, followed by an additional wash with BAL buffer and two washes with HBSS. Cells from 12-well plates were then detached in a PBS solution containing 0.1% glucose and 0.5 mM EDTA. A Bradford protein assay or cell counting was done in order to transfer equal number of cells to wells of white 96-well plates (Costar 3917).

For the intra-molecular constructs, the procedure was very similar, except that the full labeling was done in 96-well format to allow collection of BRET data on attached cells. The change from cells in suspension to attached cells was to standardize the condition of the cells across different assays as well as to reduce the amount of stress the cells undergo before assessing BRET. Twenty-four hours prior transfection, HEK 293 cells were plated in 6-well plates (Costar 3516) at a density of 2×10^5 cells/well. The following day cells were transfected with 0.5 μg of an FP construct and 1 μg of pcDNA3.1(-) for a final amount of 1.5 μg of DNA/well. The next day cells were detached with 0.25% Trypsin–EDTA (Wisent) and re-plated on poly-ornithine-coated white 96-well plates (Costar 3917) at a density of 5×10^4 cells/well. The cells were left to attach overnight and the next morning the cells were ready to be labeled. The FlAsH-EDT_2 labeling solution was prepared in the same manner as for the inter-molecular construct except that only 60 μl was prepared/well of the 96-well plate. The cells were washed with 150 μl of HBSS (Wisent) then the 60 μl of labeling solution was added per well. Plates were incubated at 37 °C for 1 h, sealed with parafilm and protected from light. Wells were then washed with 100 μl of BAL wash buffer for 10 min at 37 °C followed by an additional wash with BAL wash buffer and then a 150 μl wash with Kreb's buffer (146 mM NaCl, 4.2 mM KCl, 0.5 mM $MgCl_2$, 1 mM $CaCl_2$, 10 mM HEPES pH 7.4, 0.1% glucose). Finally, 80 μl of Kreb's buffer was added to each well and the cells were left to rest in the dark at room temperature for ~2 h. Due to the long incubation before data collection as well as the cells being attached to the plate, the assay buffer was switched to Kreb's buffer from PBS + 0.1% glucose and 0.5 mM EDTA. We have previously observed that HEK 293 cells maintain a healthy morphology in Kreb's buffer even when left overnight at ambient temperature.

2.8. BRET assay

To verify labeling efficiency, fluorescence intensity was measured using 485/20 nm excitation and 528/20 nm emission filters and a Xenon Flash lamp as a light source on a Synergy 2 multi-mode reader (Bio-Tek). For BRET1 assays where HEK 293 cells expressed a donor molecule such as FP-RLuc in combination with different FlAsH-EDT_2 labeled recombinant FP, 10 μl of 5 μM (10×) concentrated substrate coelenterazine h (Biotium) was added and luminescence was measured with a BRET1 filter set, composed of 485/20 and 528/20 filters for the Synergy 2 or F460 and F535 filters in the Victor X Light Luminescence Plate Reader (Perkin Elmer). The BRET ratios hereby obtained represent basal BRET. Net BRET was calculated by subtracting the BRET ratio obtained in the sample with unlabeled receptor from the ratio obtained in the sample of interest. In the case where ligand-induced changes were captured, time series were performed by reading through the two filters every 0.6 s for 30 s prior to injection of 10 μl of 10 μM PGF2α (1 μM final concentration) followed by reads every 0.6 s for 1 min. The change in BRET due to ligand addition (ΔBRET) was calculated by subtracting the average BRET across all reads pre-injection from the average BRET across all reads post-injection. For experiments investigating the effect of PDC113.824 on receptor conformation, cells were pretreated for 30 min with PDC113.824 diluted to 10 μM in Kreb's buffer from a 10 mM stock in ethanol prior to taking BRET readings.

Please cite this article in press as: R. Sleno et al., Methods (2015), http://dx.doi.org/10.1016/j.ymeth.2015.05.003

3. Results and discussion

3.1. Initial design and generation of inter-molecular conformation-sensitive biosensors

Our initial development focused on furthering work we undertook to study receptor dimerization where we first demonstrated the use of FlAsH as an acceptor in a BRET pair [18]. We generated three different constructs with the TC tag positioned in either the ICL3 or the C-terminus of the D4 dopamine receptor. The two TC tag positions situated in close proximity of one another in the large ICL3 of the D4 dopamine receptor demonstrated the ability to BRET with a *Renilla* luciferase-tagged β_2AR. However, one of the findings in this study was that BRET between the two receptors was not agonist-sensitive. Thus, our first goal was to attempt to improve resolution and dynamic range of changes in basal and ligand-modulated conformational landscape adopted by ICL3. To do so, we decided to focus on a GPCR with a relatively small ICL3, the receptor for prostaglandin F2α or FP. We wanted to introduce the TC tag at a higher frequency within the sequence to essentially "walk" the acceptor through ICL3. With these objectives in mind, we generated a panel of FP constructs with the TC tag "walked" at a rate of every 3 to 4 amino acids in the ICL3 sequence (Fig. 1). The initial planning called for the TC tag to be inserted at 6 different positions though only 5 were generated. The insertion of the TC tag at position 2 proved to be problematic at the level of cloning. In the end we generated 6 total constructs consisting of FP with the wild type sequence or TC tags at position 1, 3, 4, 5 or 6 in ICL3.

3.2. Validation of inter-molecular constructs: cell surface trafficking and signaling competence

For data from either signaling or conformational biosensors to be relevant and interpretable, the proteins engineered from native signaling molecules must retain their normal cellular distribution and function (see Box 1). We next verified that the introduction of the TC tag did not have an effect on surface localization of the receptor. Cells labeled with Alexa fluor 488-conjugated antibodies by means of the HA tag on the N-terminus of the receptors were assessed for cell surface fluorescence using a confocal microscope. As seen in Fig. 2A, all 5 of the TC tag-containing receptors were able to traffic to the plasma membrane at similar levels as the receptor containing the WT ICL3 sequence.

We also verified that the TC tag did not disrupt ligand-induced signaling downstream of the receptor. FP is known to induce strong ERK1/2 mitogen-activated protein kinase (MAPK) activation upon stimulation with its endogenous ligand PGF2α [19,23,24]. Cells expressing the TC-tagged constructs or the WT receptor were stimulated with 1 μM PGF2α for 5 min. As demonstrated in Fig. 2B, the receptors with a TC tag in positions 3, 4 or 5 were able to induce ERK1/2 phosphorylation in a manner similar to the WT receptor. The introduction of the TC tag at position 6 led to a loss of the ability of the receptor to activate MAPK signaling even though the receptor could still traffic to the cell surface. We did not explicitly test position 1 as although it trafficked to the surface it did not show BRET in either the inter- or intra-molecular configurations. In order for the biosensors to be used in subsequent conformational profiling, they had to meet these two core criteria, cell surface localization and signaling competence. As such the position 6 construct was not pursued further.

3.3. Inter-molecular conformation-sensors detect BRET between the two protomers of an FP homodimer

Now that we had a panel of constructs, we investigated their ability to report on conformation. We began by assessing the specificity of labeling with FlAsH (Fig. 3A). When cells were assessed for fluorescence in the absence of FlAsH labeling, the signal was very low. Comparing labeled constructs which contained the TC tag to the construct with the wild type ICL3, only marginal increases in total fluorescence were observed. We previously reported such

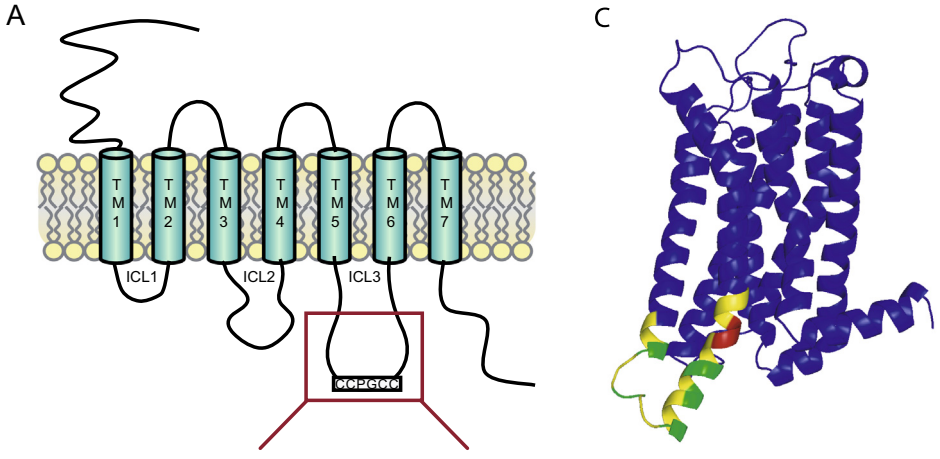

B

wild type	ITLLRVKFKSQQHRQGRSHHLEMVIQ
position 1 L227-L228	ITL CCPGCC LRVKFKSQQHRQGRSHHLEMVIQ
position 2 K231-F232	ITLLRVK CCPGCC FKSQQHRQGRSHHLEMVIQ
position 3 Q235-Q236	ITLLRVKFKSQ CCPGCC QHRQGRSHHLEMVIQ
position 4 Q239-G240	ITLLRVKFKSQQHRQ CCPGCC GRSHHLEMVIQ
position 5 S242-H243	ITLLRVKFKSQQHRQGRS CCPGCC HHLEMVIQ
position 6 E246-M247	ITLLRVKFKSQQHRQGRSHHLE CCPGCC MVIQ

Fig. 1. Constructs used for inter- and intra-molecular conformational biosensors. (A) Representation of recombinant FP. (B) ICL3 amino acid sequence indicating the different positions of the tetracysteine (TC) tag, CCPGCC motif, insertion. (C) Model of FP based on A2A crystal structure. ICL3 is colored yellow with the two amino acids flanking the TC tag positions in green for position 1 through 5 (functional sensors) or red for position 6 (non-functional sensor).

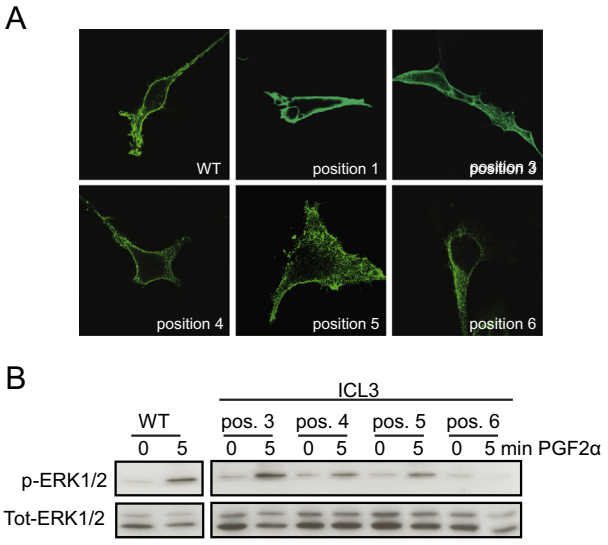

Fig. 2. Characterization of inter-molecular biosensor constructs. (A) Inter-molecular conformation-sensor constructs express receptors which traffic to the plasma membrane. Representative confocal images showing wild type HA-FP and ICL3 recombinant receptors expressed at the plasma membrane in transiently transfected HEK 293 cells. Permeabilized cells were labeled with an anti-HA primary antibody followed by an Alexa fluor 488-conjugated secondary antibody. (B) Conformation-sensors can elicit mitogen-activated protein kinase signaling upon ligand simulation. HEK 293 cells, transfected with HA-FP wild type or receptors with the CCPGCC motif inserted in the intracellular loop 3 at different positions, were stimulated with 1 μM PGF2α for 5 min. SDS–PAGE was performed on the cell lysates followed by western blot probing for phospho-ERK1/2 and total ERK1/2 as a loading control. Data shown are from single experiments in all cases.

non-specific labeling of FlAsH when measured via fluorescence alone, suggesting that many proteins may have cysteine residues in positions that allow some level of binding to the reagent [18]. However, when we assessed BRET between RLuc- and the FlAsH-tag we noted that the specificity of the signal was dramatically improved. In Fig. 3B, we observed BRET between the ICL3 of our TC-tagged FP and FP-RLuc that was TC tag position-dependent under basal conditions. Thus, our sensors were able to generate a readout of spatial proximity between two regions in an FP homodimer. We next assessed the ability of PGF2α to modulate the conformational state of the homodimer (Fig. 3C). Unfortunately, the changes in BRET due to ligand addition were highly variable and not robust enough for use in conformational profiling. Thus, we confirmed what we had noted in the earlier study of D4DR and β_2AR [18].

As these conformation-sensors were already engineered in an inter-molecular configuration, we next investigated whether other signaling proteins associated with the receptor might act as better BRET donor partners than the receptor dimer partner. We decided to focus on the heterotrimeric G proteins. We investigated BRET between the different ICL3 TC tag position constructs and a Gγ_2-RLuc construct (data not shown) [22]. Under basal conditions, no BRET was observed between Gγ_2 and the ICL3 of FP, regardless of the TC position tested (data not shown) compared to BRET between the two receptors. We also tested to see if ligand binding might modulate the receptor/G protein complex which would increase the proximity between ICL3 and Gγ_2. However, as in the receptor/receptor pair, this configuration was insensitive to ligand-induced conformational changes (data not shown).

3.4. Generation and validation of intra-molecular conformation sensitive sensors

With our limited success with the inter-molecular based conformation-sensors, we decided to pursue an intra-molecular sensor design similar to that previously reported for FRET based conformation-sensors [14,16,25–30]. These studies demonstrated that engineering TC tags into the ICL3 of the α_2AR with a CFP moiety on the C-terminus allowed capture of different ligand-specific FRET efficiencies. Our design would entail the fusion of an RLucII moiety to the C-terminus of our current line of conformation-sensors, the addition of a signal peptide to the N-terminus to further promote surface trafficking and switching to the pcDNA3.1 expression vector to boost expression levels. RLucII is a much more efficient luciferase than RLuc [8]. We also generated a construct with the previously planned position 2 of the TC tag in ICL3 in this new intra-molecular configuration (Fig. 1).

As for the inter-molecular conformation-sensors, we first functionally validated the intra-molecular sensors. We first assessed surface localization of the new panel of sensors by immunocytochemistry. In this case, the N-terminal HA tag was used to visualize surface localized sensors by labeling fixed, non-permeabilized cells. As demonstrated in Fig. 4A, all of the new conformation-sensors were trafficked to the cell surface to a similar degree as wild type FP with an RLucII moiety fused to the C-terminus. We also verified that the new constructs were still

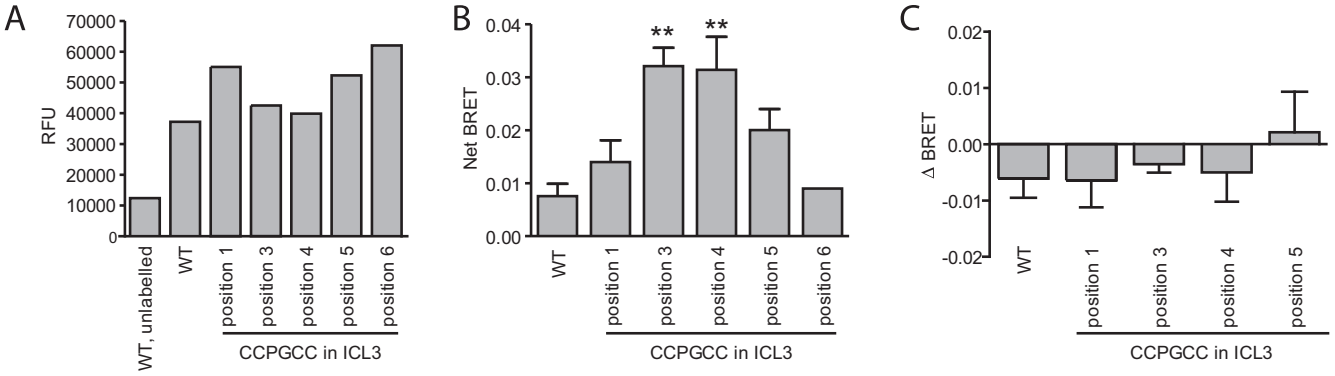

Fig. 3. Conformational profiling using inter-molecular biosensors. (A) Representative experiment showing fluorescence intensities obtained after FlAsH-EDT$_2$ labeling of HEK 293 cells transfected with FP-RLuc and CCPGCC-tagged FP. Data are expressed as relative fluorescence unit (RFU). (B) Inter-molecular (FP/FP) sensors report TC tag position-dependent BRET under basal conditions. Net BRET data shows differences in proximity between the C-tail of one protomer (FP-RLuc) and the different partner CCPGCC-tagged FP constructs. Data shown represent 3 independent experiments (with the exception for position 6 which was non-functional as a signaling-competent receptor ($n = 1$)). Statistical analysis was performed by a Dunnett's test comparing positions 1 through 5 to WT with ** denoting $p < 0.01$. (C) Inter-molecular (FP/FP) sensors do not detect ligand-induced changes in conformation. Changes in BRET ratios between FP-RLuc and the recombinant receptors following 1 μM PGF2α stimulation. Data shown were obtained from at least four different experiments. Statistical analysis was performed using one-way ANOVA but was not statistically significant at $p = 0.05$.

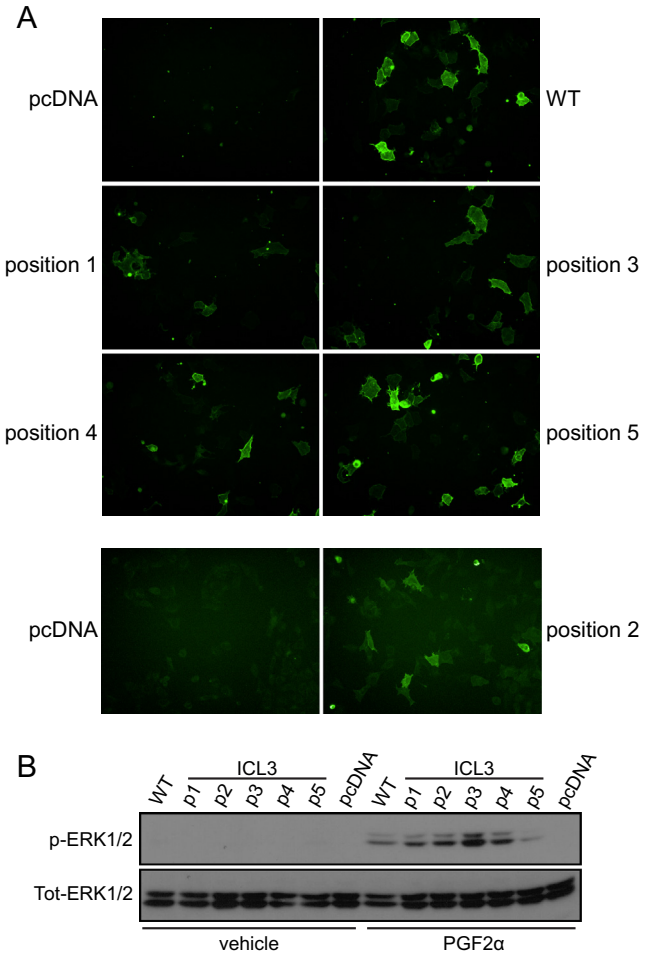

Fig. 4. Characterization of intra-molecular biosensor constructs. (A) Intra-molecular conformation-sensor constructs express receptors capable of trafficking to the plasma membrane. Immunofluorescence showing wild type SP-HA-FP-RLucII and its relative ICL3 recombinant receptors expressed on the plasma membrane in transiently transfected HEK 293 cells. Non-permeabilized cells were labeled with an anti-HA primary antibody followed by an Alexa fluor 488-conjugated secondary antibody. (B) Intra-molecular conformation-sensor constructs are functional receptors. HEK 293 cells, transfected with SP-HA-FP(WT)-RLucII or RLucII-tagged receptors with the CCPGCC motif inserted in the intracellular loop 3 at different positions, were stimulated with 1 μM PGF2α for 5 min. SDS–PAGE was performed on the cell lysates followed by western blot probing for phospho-ERK1/2 and total ERK1/2 for normalization.

capable to transmitting ligand-induced signals (Fig. 4B). Assessing MAPK activation by measuring ERK1/2 phosphorylation showed that all of the sensors could transmit a signal to some degree. Though the TC position 5 sensors could signal, it was noticeably weaker than the WT ICL3 construct even though it demonstrated similar surface expression levels by immunocytochemistry. Here, as proof of concept, we only used transient transfection, but the construction of clonal stable cell lines for the different conformational biosensors would likely normalize both surface localization and signaling.

3.5. Intra-molecular conformation-sensitive sensors capture ligand-induced conformational changes

With the transition from the inter- to intra-molecular configuration, as well as changing to the brighter RLucII variant, we were able to substantially increase the net BRET observed under basal conditions with the sensors (Fig. 5A). As with the original panel, net BRET was TC tag position-dependent with a similar rank-order of the positions where those near the middle of the loop generated the highest BRET. We next assessed the ability of the intra-molecular conformation sensors to capture ligand-induced changes. PGF2α-induced changes in basal BRET were observed in 3 out the 5 sensors, with the conformational change in the position 4 sensor being significant across 4 independent experiments (Fig. 5B). This decrease in BRET seen at the position 4 sensor would suggest that upon receptor activation the C-terminus and ICL3 separate. This change in BRET at position 4 was also dose-dependent (data not shown) which is a critical step in the validation of ligand effects.

It should be possible to improve the resolution of conformational changes captured in response to ligands or protein partners by increasing the coverage of the sensors by using smaller probes compared to the six amino acid TC tag insertion. This could be done by using a scan for each residue, replacing them with single unnatural amino acids [31–33] and labeling them through some variety of click chemistry. It is likely that single amino acid substitutions would be better tolerated than the TC sequence we used. This might result in a finer map of conformational dynamics but would complicate analysis as additional cDNAs for the tRNA synthase and the tRNA would be required. Surprisingly, even a small number of TC probes were sufficient to observe the dynamics of receptor activation from distinct conformational vantage points. Engineering a limited number of such probes into the other intracellular loops and the carboxy-tail would likely add to the discriminatory power

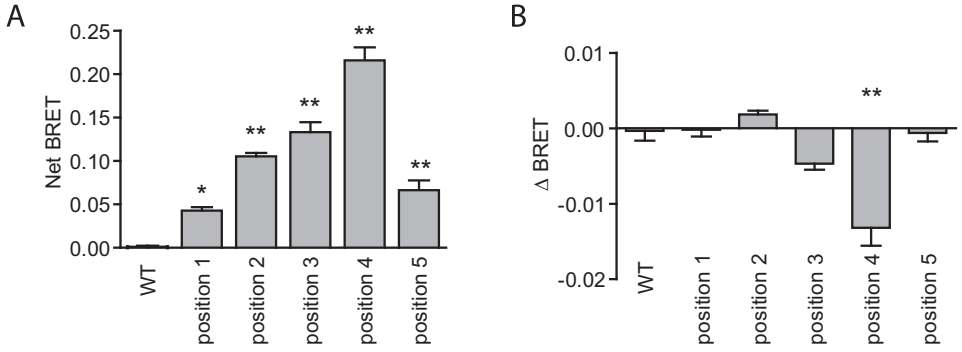

Fig. 5. Conformational profiling using intra-molecular biosensors. (A) Intra-molecular sensors report TC tag position-dependent BRET under basal conditions. Net BRET data between the C-tail (RLucII) and the ICL3 of the CCPGCC-tagged FP constructs. At least two independent experiments are shown. Statistical analysis was performed by a Dunnett's test comparing position 1 through 5 to WT with * denoting $p < 0.05$ and ** denoting $p < 0.01$. (B) Intra-molecular sensors detect ligand-induced changes in receptor conformation. Stimulation with 1 μM PGF2α leads to changes in the relative position between the C-terminus and ICL3 for 3 different sensors. Data represent at least three different experiments. Statistical analysis was performed by a Dunnett's test comparing position 1 through 5 to WT with ** denoting $p < 0.01$.

by increasing the number of relevant vantage points. One could also imagine such "walks" on the exterior of the receptor using a labeled ligand as a FRET partner. Another possibility would be to engineer smaller versions of luciferase that are BRET-competent, such as Nano-Luc [34] into different positions such as the N-terminus or the intracellular or extracellular loops. Some studies have shown that GPCRs can tolerate large adducts in ICL3 [15] but care should be taken in these cases to undertake the validation steps outlined in Box 1.

3.6. An allosteric modulator of FP has a cell density-dependent effect on receptor conformation

PDC113.824 has been previously characterized as a positive allosteric modulator (PAM) of $G\alpha_q$ signaling and a negative allosteric modulator (NAM) of $G\alpha_{12}$ signaling when the FP binds PGF2α [19,24]. This compound is an ECL2 peptidomimetic which likely has a very low affinity for FP and the only way to measure its effects easily have relied on ligand binding dissociation kinetics. Since our intra-molecular sensors could capture PGF2α-induced conformational changes between ICL3 and the C-terminus, we next tested to see whether the presence of PDC113.824 could modulate that signal. We decided to focus on the position 4 sensor since it had the largest dynamic range of our panel. Our initial experiments involved pre-incubation with PDC113.824 followed by the standard procedure we used to collect vehicle- or PGF2α-induced changes in BRET. However, after performing the experiment multiple times we noted a large variability in the effect on conformation driven by PGF2α with some experiments producing a strong potentiation of the response to PGF2α while in other cases the response was reduced (data not shown). We next tested multiple factors such as the expression level of the sensor, the requirement for co-expression of stoichiometric amounts of G protein partners and finally the density of plated cells. There was a clear trend ranging from repression to potentiation as the density of cells was increased from 1×10^4 to 1×10^5 cells/well (Fig. 6). Our previous experiment was run with a density of 5×10^4 cells/well which is right at the tipping point between these two effects of PDC113.824, which might explain the lack of reproducibility in the standard experiment.

Taken together, our results demonstrate the utility of focusing on GPCR conformation, rather than downstream signaling events *per se*. Our conformational biosensors should work in any cell, be sensitive to both orthosteric or allosteric ligands, be they small molecules or interacting proteins as well as changes in cell environment, i.e. membrane lipid composition of compartmentalization. Unlike signaling signatures, they do not need to be reinvented each time the investigator moves to a different cell or tissue type. The portability of such receptor-proximal biosensors should make them an interesting and useful adjunct to signal profiling and help stratify ligands beforehand.

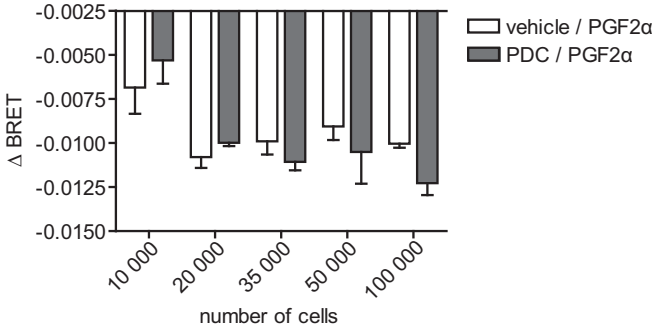

Fig. 6. The effect of the allosteric modulator PDC113.824 on FP conformation is dependent on cell density. HEK 293 cells transiently transfected with the SP-HA-FP-ICL3 P4-RLucII sensor were plated at different densities in the well of a 96-well plate. After labeling with FlAsH-EDT_2, cells were pre-treated with 10 μM PDC 113.824 for 30 min prior to measuring the effects of 1 μM PGF2α on receptor conformation ($n = 2$).

Box 1 Validating biosensors.

These are general considerations. More specific consideration might include co-expression of particular accessory proteins (as in the case of G protein assays which require additional constructs beyond the basic BRET pair).

Initial issues-validating constructs

(1) Are constructs validated by restriction digestion and bidirectional sequencing?
(2) Are the tagged constructs for BRET functional in ways comparable to untagged proteins?
(3) Are tagged constructs localized correctly in the cell under basal conditions?
(4) Are tagged constructs localized correctly in the cell following stimulation by receptor ligands?
(5) Are any necessary accessory constructs which must be co-transfected with basic assay components validated as in steps 1–4?

Issues for scale up

(6) Can the basic assay be reliably performed in a 96-well plate?
(7) Can biosensor cell lines be made stable and clonal?
(8) Measurement of dynamic range of the assay. This should meet certain minimum criteria for HTS
(9) Is the assay portable from cell type to cell type?
(10) Does the assay require minimal manipulation, and the instrumentation and reagents needed for reading the signal should be relatively inexpensive?
(11) The assay should be easily quantifiable using standard data handling software

Acknowledgments

This work was supported by a grant from the Consortium Québécois sur la Découverte du Médicament and the Canadian Institutes of Health Research (CIHR, MOP-130309). RS was supported by a scholarship from the McGill-CIHR Drug Development Training Program. We thank Vic Rebois for many helpful discussions regarding the initiation of this work. We thank William Lubell for the generous gift of PDC113, 824.

References

[1] T. Kenakin, A. Christopoulos, Nat. Rev. Drug Discov. 12 (6) (2013). 483–483.
[2] T. Kenakin, A. Christopoulos, Nat. Rev. Drug Discov. 12 (3) (2013) 205–216.
[3] I. Charfi et al., Br. J. Pharmacol. 172 (2) (2014) 435–448.
[4] E.T. van der Westhuizen et al., Mol. Pharmacol. 85 (3) (2014) 492–509.
[5] J. Corbisier et al., J. Biol. Chem. (2015).
[6] A. Salahpour et al., Front. Endocrinol. 3 (2012).
[7] A. Saulière et al., Nat. Chem. Biol. 8 (7) (2012) 622–630.
[8] R. Carr et al., J. Biol. Chem. 289 (52) (2014) 35668–35684.
[9] T. Kenakin, F1000 Biol. Rep. 1 (2009) 87.
[10] V. Katritch, V. Cherezov, R.C. Stevens, Annu. Rev. Pharmacol. Toxicol. 53 (1) (2013) 531–556.
[11] R. Nygaard et al., Cell 152 (3) (2013) 532–542.
[12] B.K. Shoichet, B.K. Kobilka, Trends Pharmacol. Sci. 33 (5) (2012) 268–272.

[13] M.J. Lohse, S. Nuber, C. Hoffmann, Pharmacol. Rev. 64 (2) (2012) 299–336.
[14] C. Hoffmann et al., Nat. Protoc. 5 (10) (2010) 1666–1677.
[15] J.-P. Vilardaga et al., Nat. Biotechnol. 21 (7) (2003) 807–812.
[16] N. Ziegler et al., Bioorg. Med. Chem. 19 (3) (2011) 1048–1054.
[17] N. Boute, R. Jockers, T. Issad, Trends Pharmacol. Sci. 23 (8) (2002) 351–354.
[18] R.V. Rebois et al., Cell. Signal. 24 (11) (2012) 2051–2060.
[19] E. Goupil et al., J. Biol. Chem. 285 (33) (2010) 25624–25636.
[20] L.A. Kelly, S. MJE, Nat. Protoc. 4 (2009) 363–371.
[21] E. Goupil et al., J. Biol. Chem. 290 (5) (2015) 3137–3148.
[22] R.V. Rebois et al., J. Cell Sci. 119 (13) (2006) 2807–2818.
[23] E. Goupil et al., Mol. Endocrinol. 26 (7) (2012) 1189–1202.
[24] C.B. Bourguet et al., J. Med. Chem. 54 (17) (2011) 6085–6097.
[25] A. Gautier et al., in: Site-Specific Protein Labeling, Springer, New York, 2014, pp. 1–6.
[26] J. Nakanishi et al., Biochem. Biophys. Res. Commun. 343 (4) (2006) 1191–1196.
[27] C. Hoffmann et al., Nat. Methods 2 (3) (2005) 171–176.
[28] A. Zürn et al., Mol. Pharmacol. 75 (3) (2009) 534–541.
[29] J.-P. Vilardaga et al., Nat. Chem. Biol. 4 (2) (2008) 126–131.
[30] M. Maier-Peuschel et al., J. Biol. Chem. 285 (12) (2010) 8793–8800.
[31] S. Naganathan et al., Biochemistry 54 (3) (2015) 776–786.
[32] T. Huber, P. Thomas, Chem. Biol. 21 (9) (2014) 1224–1237.
[33] H. Tian et al., ChemBioChem 15 (12) (2014) 1820–1829.
[34] A.C. Stacer et al., Mol. Imaging 12 (7) (2013) 1–13.

Please cite this article in press as: R. Sleno et al., Methods (2015), http://dx.doi.org/10.1016/j.ymeth.2015.05.003